PERGAMON

Vision Research 42 (2002) 2447–2455

Vision Research

www.elsevier.com/locate/visres

The importance of spatial scale in determining illusions of orientation

Jennifer Skillen [a,*], David Whitaker [a], Ariella V. Popple [b], Paul V. McGraw [a]

[a] Department of Optometry, University of Bradford, Richmond Road, Bradford BD7 1DP, UK
[b] Optometry, Minor Hall, University of California, Berkeley, CA 94720-2020, USA

Received 4 October 2001; received in revised form 19 June 2002

Abstract

The twisted-cord illusion is a powerful demonstration of interaction between 1st-order (luminance-defined) and 2nd-order (contrast-defined) orientation processing. The perceived orientation of contrast-defined objects is pulled towards their 1st-order orientation content when the difference in orientation is small (Fraser effect), yet is pushed away from the 1st-order content at large orientation differences (Zöllner effect). Here we show that the relative spatial scale of carrier and envelope represents a decisive factor in determining the magnitude and direction of such interactions. We conclude that the perceived 2nd-order structure of a stimulus is biased by the properties of the 1st-order structure in a manner that depends on relative, rather than absolute spatial scale.

Keywords: 1st-order; 2nd-order; Orientation; Spatial scale; Illusion

1. Introduction

Human sensitivity to variations in luminance within a visual scene is consistent with neurophysiological observations that the mammalian visual system contains simple neurons which signal the difference in average luminance between the excitatory and inhibitory regions of their receptive field in a linear fashion (DeValois, Albrecht, & Thorell, 1982; Hubel & Weisel, 1959; Movshon, Thompson, & Tolhurst, 1978). However, a large proportion of neurons signal more complex properties of the visual scene which can often be understood on the basis of pooling of a number of inputs in a non-linear manner (von der Heydt & Peterhans, 1989; Shapley, 1994; Spitzer & Hochstein, 1985). This neurophysiological behaviour offers a potential explanation for the many varieties of human visual percepts that are inconsistent with purely linear processing. Consider, for example, the pairs of horizontal cords in Fig. 1. These contain internal structure (known as '1st-order' structure) consisting of alternating dark and light stripes that, individually, are ideally suited to analysis by a linear neuron centred upon either a light or dark stripe. The cord as a whole, however, contains no net variation in luminance relative to the surround, and would therefore be invisible to a linear neuron which averaged luminance across its receptive field. Nevertheless, each cord is clearly perceived as having a global structure (known as '2nd-order' structure), allowing analysis of its orientation and shape. This could be consistent with a percept based upon the output of a horizontally oriented neuron, which collated the output of smaller, linear neurons along the length of the cord independently of their polarity. Models of 2nd-order visual processing include an initial stage of linear filtering, followed by a non-linear stage (full- or half-wave rectification) and a subsequent filtering stage at a relatively coarse spatial scale (Badcock & Derrington, 1985; Burton, 1973; Chubb & Sperling, 1988; Henning, Hertz, & Broadbent, 1975; Morgan & Baldassi, 1997; Morgan, Mason, & Baldassi, 2000; Sutter, Sperling, & Chubb, 1995; Wilson, Ferrera, & Yo, 1992).

The picture therefore emerges of two streams of visual processing—a 1st-order stream dealing with the analysis of luminance variations within a scene, and a 2nd-order stream dealing with variations in contrast or texture, but which itself receives an initial input from linear, 1st-order neurons. Both types of mechanism are known to subserve a variety of visual tasks, such as motion perception (Chubb & Sperling, 1988;

* Corresponding author.
E-mail address: j.skillen@bradford.ac.uk (J. Skillen).

0042-6989/02/$ - see front matter
PII: S0042-6989(02)00261-4

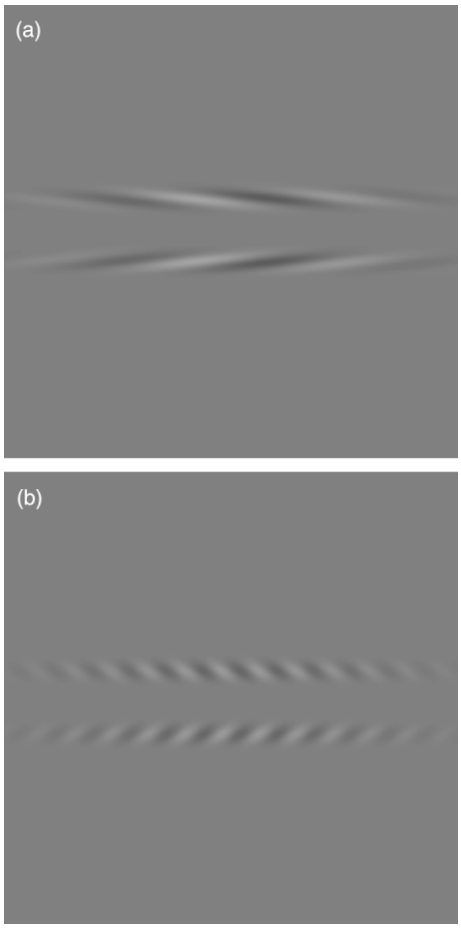

Fig. 1. Examples of the twisted-cord stimuli. The global orientation (envelope) of each cord is influenced by the orientation of the local structure (carrier) to produce two very different effects. In (a) the pair of cords appear to converge to the right since the perceived orientation of the envelope is tilted in the same direction as the carrier information—the Fraser effect. The carrier tilt is 10°. In (b), the envelope appears tilted in the opposite direction to that of the carrier tilt—the Zöllner effect. The carrier tilt is 50°. The cords now appear converged to the left. For demonstration purposes this figure is presented at a higher contrast level (0.5) than was used in the experiment (0.1).

Edwards & Badcock, 1995; Ledgeway & Smith, 1994), spatial position (McGraw, Levi, & Whitaker, 1999; Whitaker, McGraw, & Levi, 1997) and depth perception (Langley, Fleet, & Hibbard, 1999; Zeigler & Hess, 1999), as well as curvature and orientation perception (Dakin, Williams, & Hess, 1999; Lin & Wilson, 1996; Morgan & Baldassi, 1997; Morgan et al., 2000; Smith, Clifford, & Wenderoth, 2001; Wilson & Richards, 1992).

There is no a priori reason why the output of the 2nd-order system should be influenced by the nature of the 1st-order structure from which it receives its input. Neurophysiological studies indicate that individual 2nd-order filters are tuned to a narrow range of 1st-order spatial frequencies and orientations, and there is not a strict relationship between these 1st-order characteristics and the spatial frequency or orientation tuning of the 2nd-order filter (Mareschal & Baker, 1998; Zhou & Baker, 1996). Pooling of the output of 2nd-order neurons with common tuning properties, yet with markedly dissimilar 1st-order inputs would produce a system which responded to 2nd-order structure independently of its origin. There is evidence for such a pooling process in the orientation domain (McGraw et al., 1999; Wenderoth, Clifford, & Wyatt, 2001) although the extent of pooling across spatial frequency is more contentious (Dakin & Mareschal, 2000; McGraw et al., 1999).

Nevertheless, a variety of striking visual illusions, which have been the subject of investigation for over a century, suggest very strongly that the perceptual output of the 2nd-order stream can be strongly biased by the nature of the 1st-order structure from which it is derived. Fig. 1a is an example of the stimuli used in the study which shows the Fraser Twisted-cord illusion. Each of the two cords is made up of a tilted 1st-order luminance modulation (henceforth called the 'carrier') along the length of the cord, yet the global orientation of each cord (henceforth called the 'envelope') remains horizontally oriented. It should be clear, however, that the perceived orientation of the envelope is not horizontal, but is biased in the direction of the carrier orientation such that the cords appear to be converging towards the right-hand side of the figure—the Fraser illusion. The Fraser illusion usually occurs when the orientation of the internal structure is less than 10–15° relative to the orientation of the overall cord (Fraser, 1908). If the orientation of the local elements exceeds 10–15° (Fig. 1b) the cords are seen tilted in the opposite direction. This reversed effect is called the Zöllner illusion.

Illusions such as the one demonstrated in Fig. 1 offer considerable potential to examine the nature of the relationship between 1st- and 2nd-order visual structure. However, previous studies using this type of stimulus have produced results that have been difficult to reconcile with commonly accepted models of 2nd-order visual processing (Dakin et al., 1999). In the present study, we demonstrate the critical importance of the spatial scale relationship between 1st- and 2nd-order spatial structure, and examine its implications for models of 2nd-order visual processing.

2. Methods

2.1. Stimuli

Each stimulus comprised two cords with each cord consisting of a luminance-defined sinusoidal carrier grating (1st-order information) windowed by a horizontally elongated Gaussian envelope (2nd-order infor-

mation) with an aspect ratio of 18:1. The mathematical description of these stimuli is given by

$$L_{\text{mean}} + L_{\text{mean}} C \sin(2\pi F(x\sin\theta + y\cos\theta) + \phi) \times \exp\left[\frac{-x^2}{2\sigma_{x^2}} + \frac{-y^2}{2\sigma_{y^2}}\right] \quad (1)$$

where L_{mean} is the mean luminance of the background (22.6 cd m^{-2}), C is the stimulus contrast (which was maintained at 0.1) and F is the spatial frequency of the carrier grating whose orientation is θ. The vertical and horizontal distances from the peak of the Gaussian envelope of each cord are denoted by x and y. The phase of the carrier grating, ϕ, was maintained at zero in order to minimise the introduction of mean luminance cues to the 2nd-order stimuli. The vertical and horizontal standard deviations (σ_y and σ_x) of the Gaussian envelope of each cord were 9′ and 162′, respectively. Carrier-induced distortions in the perceived tilt of the envelope were offset by physically rotating each of the cords as a whole, as described in '*Procedures*' below.

Stimuli were presented for 200 ms on a 20-inch electron d2 monitor. The non-linear luminance response of the display was linearised by using the inverse function of the luminance response as measured using a Minolta CS-100 photometer. The host computer was a Starmax 4000/200. The contrast resolution of the monitor was increased to 12-bit using a video summation device constructed according to Pelli and Zhang (1991). All stimuli were generated using the macro capabilities of the public domain software NIH image™ 1.59 (developed by the US National Institutes of Health and available from the Internet by anonymous FTP from zippy.nimh.nih.gov).

2.2. Procedures

A two alternative forced-choice paradigm was used in which subjects were required to make a judgement on whether the two central cords within a display were seen to converge to the right or to the left (Fig. 1a and b). The envelopes of the two cords could be presented at any one of seven orientations spaced around an approximate zero position indicated by an initial method of adjustment. Subsequent presentations by the method of single stimuli included a total of 40 trials presented at each of the seven levels. On any trial either the stimulus or its horizontal mirror-image could be presented. This ensured that the subject's left–right responses were close to 50:50 even if the initial method of adjustment estimate was imperfect. Subject responses to the perceived tilt or curvature of the cords were recorded for each of the seven levels. Resulting psychometric functions were fitted using a logistic function to reveal the point of subjective equality (50% response level) and the threshold (half the difference between 27% and 73% response levels). Functions were discarded if they failed to span the 15–85% range approximately, usually as a result of a biased initial estimate of zero position. The data were then recollected using a new method of adjustment estimate.

2.3. Observers

Data are presented for two of the authors and is representative of similar findings for a naïve subject. Each subject had normal or corrected to normal distance acuity. Observations were made within a dimly lit room under binocular viewing conditions.

3. Results

3.1. Experiment 1: dependence of perceived envelope structure upon carrier spatial frequency

Fig. 2 shows the effect on perceived envelope structure of changing carrier spatial frequency for two subjects. Envelope size ($\sigma_x = 162'$, $\sigma_y = 9'$) was kept constant whilst carrier spatial frequencies of 0.75, 1.5, 3.0 and 6.0 c deg^{-1} were compared. Curve fits to the data, shown in Fig. 2, represent the best fit of a function which considers the perceived orientation of the envelope (r_{env}) to be a weighted mean of its true orientation (θ_{env}) and an orientation–dependent input from the carrier (θ_{car}):

$$r_{\text{env}}(\theta_{\text{car}}) = (\theta_{\text{env}} + \theta_{\text{car}}(A e^{-(\theta_{\text{car}}-\theta_{\text{env}})^2/2\sigma_{\text{E}}^2} - B e^{-(\theta_{\text{car}}-\theta_{\text{env}})^2/2\sigma_{\text{I}}^2}))/2 \quad |-90 < (\theta_{\text{car}} - \theta_{\text{env}}) < 90| \quad (2)$$

where A and B are the respective amplitudes of excitatory and inhibitory Gaussian contributions due to the carrier orientation, and σ_{E} and σ_{I} are the standard deviations (halfwidths) of the same. If we restrict our consideration to horizontally oriented envelopes ($\theta_{\text{env}} = 0$), this simplifies to

$$r_{\text{env}}(\theta_{\text{car}}) = \theta_{\text{car}}(A e^{-\theta_{\text{car}}^2/2\sigma_{\text{E}}^2} - B e^{-\theta_{\text{car}}^2/2\sigma_{\text{I}}^2})/2 \quad |-90 < \theta_{\text{car}} < 90| \quad (3)$$

The data is fitted with Eq. (3), with the four free parameters A, B, σ_{E} and σ_{I} allowed to float to produce a best fit for each spatial frequency data set. Previous studies have used curve fits of this type to describe cross-orientation interaction (Blakemore, Carpenter, & Georgeson, 1970; Paradiso, 1988; Ringach, 1998; Tyler & Nakayama, 1984). Furthermore, functions of this type have also been used to describe physiological data (Blakemore & Tobin, 1972; Ferster, 1986), and to develop physiologically plausible models of cross-orientation interaction (e.g. Paradiso, 1988).

As the carrier spatial frequency content changes from low to high (Fig. 2) it is clear that the magnitude of

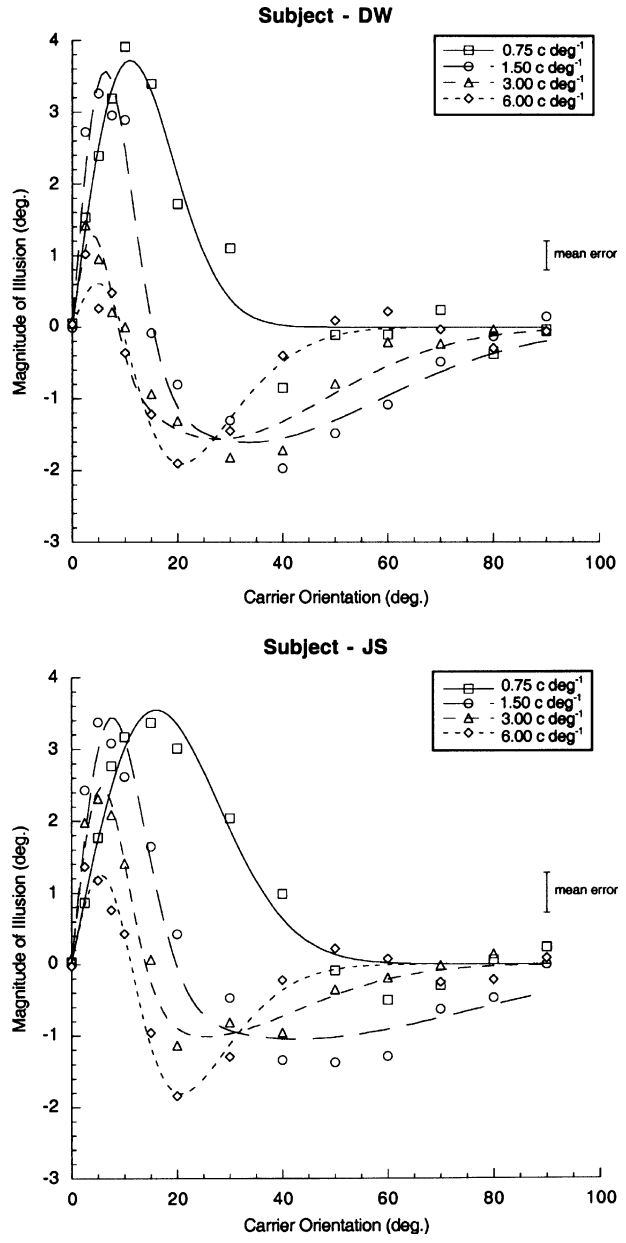

Fig. 2. The effect of changing carrier spatial frequency on the perceived envelope orientation for two subjects. Carrier spatial frequencies of 0.75 c deg^{-1} (squares), 1.5 c deg^{-1} (circles), 3.0 c deg^{-1} (triangles) and 6.0 c deg^{-1} (diamonds) were investigated. The 0.75 c deg^{-1} condition results exclusively in an attraction of the envelope in the direction of the carrier (Fraser effect). As carrier frequency increases the magnitude of the Fraser effect reduces as the repulsive Zöllner effect grows. Each data set has been fitted with Eq. (3). Error bars represent 95% confidence limits.

Fraser illusion decreases in conjunction with a corresponding increase in the magnitude of the Zöllner effect. Our mid frequency plots are consistent with several previous studies which have used similar stimuli (Dakin et al., 1999; Morgan & Baldassi, 1997; Morgan et al., 2000; Tyler & Nakayama, 1984). For small carrier orientations (0–20°) a positive bias occurs, reflecting the well-established Fraser effect in which the carrier attracts the orientation of the envelope. However, for larger carrier grating orientations (20–80°) the misperception is reversed so that the envelope is now perceived oriented in the opposite direction to its carrier features (Zöllner effect). Very different effects are found at lower and higher frequencies. At low spatial frequencies (0.75 c deg^{-1}) a large Fraser effect occurs over much of the orientation range, and no significant Zöllner effect is found. The opposite is true for the highest spatial frequency condition tested (6 c deg^{-1}) in which the envelope is predominantly perceived as tilted in the direction opposite to the carrier (Zöllner effect), with only a small Fraser effect at the lowest carrier orientations.

The four parameters from the curve fits are shown in Table 1 for each of the spatial frequencies tested. The amplitude of the excitatory component shows a shallow band-pass tuning with respect to the spatial frequency of the carrier, whereas the inhibitory component demonstrates a much more significant dependence upon spatial frequency. At high frequencies its amplitude approaches that of the excitatory component, but as spatial frequency is reduced its amplitude falls to zero. This is reflected in the absence of any Zöllner (repulsion) effect for the lowest spatial frequency data in Fig. 2. The halfwidth of the inhibitory component is consistently broader than that of the excitatory component.

Fig. 3 demonstrates changes in *thresholds* rather than bias. Thresholds for each spatial frequency condition demonstrated no systematic differences, and we have therefore presented mean thresholds, averaged across spatial frequency. Envelope judgements are most accurate (thresholds of approximately 0.2°) when the carrier is parallel to the envelope. Thresholds increase rapidly as the carrier orientation moves away from that of the envelope, reaching a peak at orientations around 20° before gradually decreasing again to the point where the carrier is orthogonal to the envelope. This finding is similar to that of Lin and Wilson (1996) who showed that envelope orientation thresholds are higher for oblique carriers compared to horizontal carriers. It is also qualitatively similar to the effect of carrier orientation on envelope orientation thresholds found by Dakin et al. (1999), although the lower thresholds in the present study can be attributed to our use of longer, thinner envelopes which allow for more accurate orientation judgements. A simple explanation for these threshold effects is that both the 1st-order and 2nd-order signals possess trial-to-trial variations in strength due to internal noise. At the stage where 1st-order signal interferes with the 2nd-order judgement, the percept will depend upon the relative strength of the two orientation signals. When the two signals are consistent (i.e. when the carrier orientation is identical to that of the envelope) this will have no detrimental effect. When they are disparate, however, the result will be an increase in variability of

Table 1
Amplitude and halfwidth of the excitatory and inhibitory components of the curve fit of Eq. (3) as a function of spatial frequency for both subjects

Subject	Spatial frequency (c deg^{-1})	Excitatory		Inhibitory	
		Amplitude of Gaussian (deg)	Halfwidth of Gaussian (deg)	Amplitude of Gaussian (deg)	Halfwidth of Gaussian (deg)
DW	0.75	1.12 ± 0.10	10.95 ± 0.61	0	–
	1.50	2.03 ± 0.17	6.62 ± 0.041	0.16 ± 0.03	33.51 ± 3.43
	3.00	1.25 ± 0.24	4.40 ± 0.48	0.19 ± 0.03	27.81 ± 2.22
	6.00	0.83 ± 0.15	7.31 ± 1.40	0.43 ± 0.17	16.63 ± 2.12
JS	0.75	0.73 ± 0.06	16.0 ± 0.61	0	–
	1.50	1.55 ± 0.16	8.01 ± 0.60	0.08 ± 0.03	43.03 ± 8.71
	3.00	1.54 ± 0.12	6.16 ± 0.35	0.14 ± 0.03	24.66 ± 2.78
	6.00	1.20 ± 0.17	7.28 ± 1.00	0.47 ± 0.20	15.66 ± 2.05

Standard errors of the parameters are also provided. See text for further details.

the orientation percept from trial-to-trial, hence an increase in threshold.

3.2. Experiment 2: scale invariance of the effect

Fig. 4 shows the effect of joint manipulation of the spatial frequency content of the carrier and the spatial characteristics of the envelope for two subjects. The stimulus was the same as the 1.5 c deg^{-1} carrier frequency condition used in the previous experiment. Four different viewing distances (0.575, 1.15, 2.30 and 4.60 m) were employed to examine the extent to which scale invariance holds for the task. The magnitude of the orientation misperceptions (Fig. 4) showed no clear dependence upon viewing distance. For this reason, the data for all four viewing distances are fitted with a single function (Eq. (3)), the parameters of which agree well with the corresponding data set from the previous spatial frequency experiment (see Fig. 4 legend). Threshold data for the four viewing distances each demonstrated a similar trend and mean thresholds, averaged across distance, are shown in Fig. 5. Changes in threshold as a function of carrier orientation are consistent with those shown in Fig. 3. We conclude that the magnitude and direction of illusion demonstrates scale invariance by remaining independent of viewing distance. This implies that the important parameter in determining the frequency effects shown in Fig. 2 is not the spatial frequency content of the carrier per se but its spatial scale in relation to that of the envelope.

4. General discussion

In line with previous studies (Dakin et al., 1999; Morgan & Baldassi, 1997; Morgan et al., 2000; Popple & Levi, 2000; Tyler & Nakayama, 1984) our data demonstrate interactions between the processing of 1st-order (luminance-defined) and 2nd-order (contrast-defined) information within the orientation domain. We have also found similar effects in the curvature domain, by varying the relative curvature of carrier and envelope. Fig. 6a and b represent a striking demonstration within the curvature domain of the main findings of the present study—that interaction effects between carrier and envelope depend upon the relative spatial scale of the two. Both figures represent a radial carrier grating of relatively low (Fig. 6a) or high (Fig. 6b) spatial frequency whose contrast is windowed by a series of squares. As the radial spatial frequency of both gratings increases towards the centre of the figures, so the size of the square windows decreases in exact relationship. Since both radial gratings share a common origin at the centre of their respective figures, at any given point the curvature of the low spatial frequency grating is identical to that of the higher frequency grating. When the scale of the carrier is large relative to that of its envelope (Fig. 6a), strong attractive effects are found, in the direction of the traditional Fraser illusion. This results in a 'bowing out' of the edges of the square boxes in a convex direction. On the other hand, when the scale of the carrier is small relative to the envelope, the perception is consistent with repulsive effects such as that found in the traditional Zöllner illusion (Fig. 6b). This results in the edges of the boxes being 'bowed inwards' in a concave direction.

The findings of our experiments are clear-cut. The global misperceptions of orientation induced by 1st-order carrier structure are critically dependent upon the relative scale of carrier (defined by its spatial period) and envelope (defined by its σ_y). It is injudicious, therefore, to make statements concerning the orientation range over which attraction and repulsion effects occur without considering the issue of spatial scale. At one extreme, when the scale of the carrier is coarse relative to that of the envelope, the interaction effect is entirely attractive. At the other extreme, when the carrier scale is fine relative to the envelope, repulsion effects dominate. It is also potentially confounding to examine the issue of relative spatial scale at a single orientation value. For example, a snapshot of the data in Fig. 2 at an abscissa

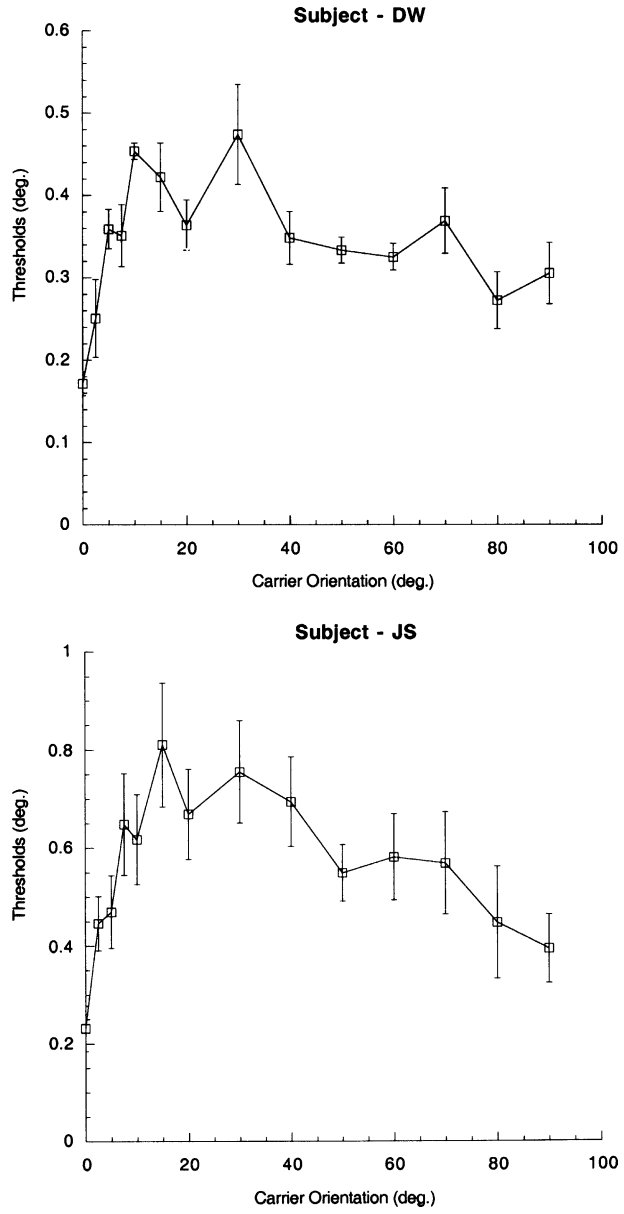

Fig. 3. Mean thresholds for both observers as a function of carrier orientation, averaged across the four carrier spatial frequencies. Error bars represent the standard error of the mean. The data reveals that performance is optimum when the carrier is orthogonal or perpendicular to the envelope. See text for further details.

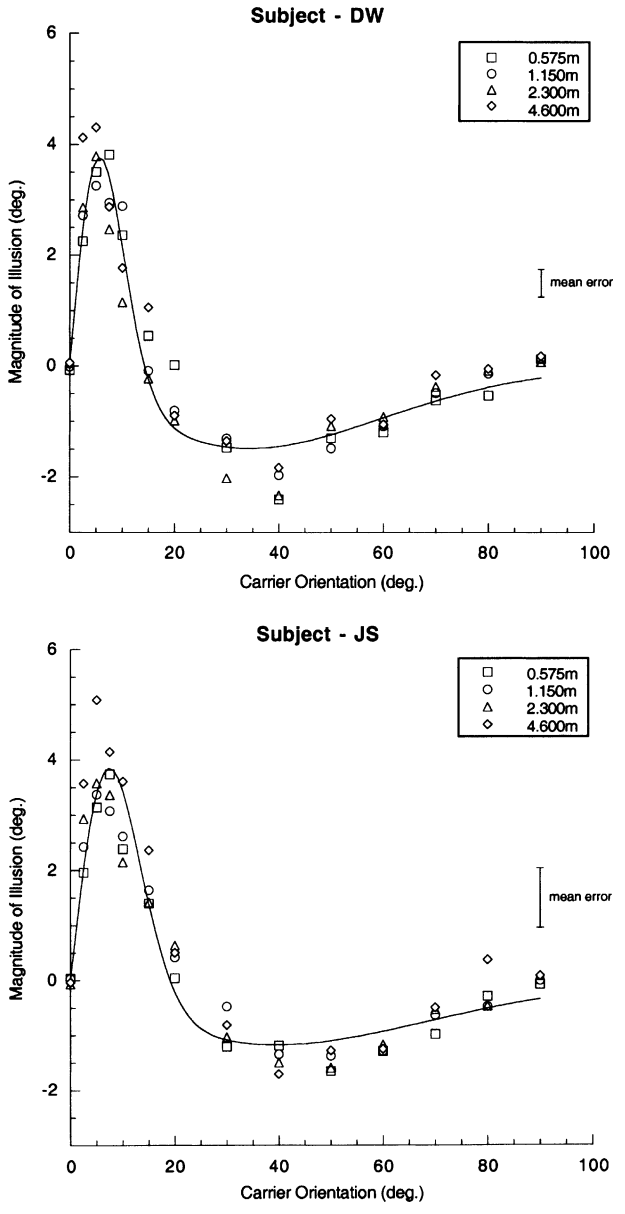

Fig. 4. The effect of changing the carrier spatial frequency in a fixed spatial relationship to that of the envelope is shown for two subjects. The following denotes the different viewing distances: 0.575 m (squares), 1.15 m (circles), 2.30 m (triangles), and 4.60 m (diamonds). Curve fits represent the best fit of Eq. (3) to the data across all four viewing distances. Parameters of the curve fit are $A = 2.31°$, $B = 0.142°$, $\sigma_E = 5.97°$ and $\sigma_I = 34.4°$ (DW); $A = 1.79°$, $B = 0.10°$, $\sigma_E = 7.76°$ and $\sigma_I = 39.7°$ (JS).

value of 20° would provide a very different pattern of results to those at, say, 50°. Nevertheless, the data of previous studies that have varied the spatial frequency of the carrier relative to a fixed envelope is consistent with our results shown in Fig. 2. Tyler and Nakayama (1984) examined the perceived global tilt of a bar consisting of a series of tilted lines. By varying the number of tilted lines within a fixed bar length, they investigated changes in attractive effects (at a line tilt of 15°) and repulsive effects (at a line tilt of 40°). Both effects were found to decrease with an increasing number of lines. At 15° of carrier orientation, our data shown in Fig. 2 are consistent with a reduction in Fraser effect with increasing carrier frequency. At 40° a reduction in the Zöllner effect can also be seen, at least between carrier frequencies of 1.5–6 c deg^{-1}. This latter effect has also been demonstrated by Dakin et al. (1999) using a range of carrier frequencies within a fixed envelope at a single carrier orientation of 45°. McOwan and Johnston (1996) investigated a related stimulus consisting of an oblique sinusoidal contrast modulation of a luminance grating.

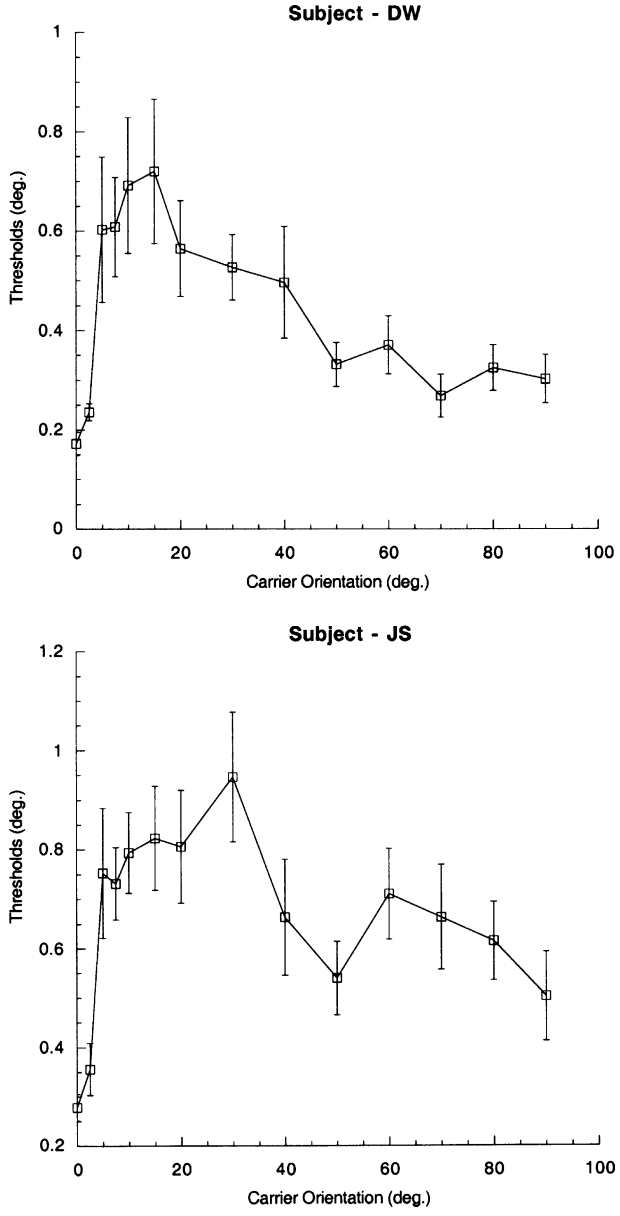

Fig. 5. Mean thresholds for both observers as a function of carrier orientation, averaged across the four viewing distances. Error bars represent the standard error of the mean.

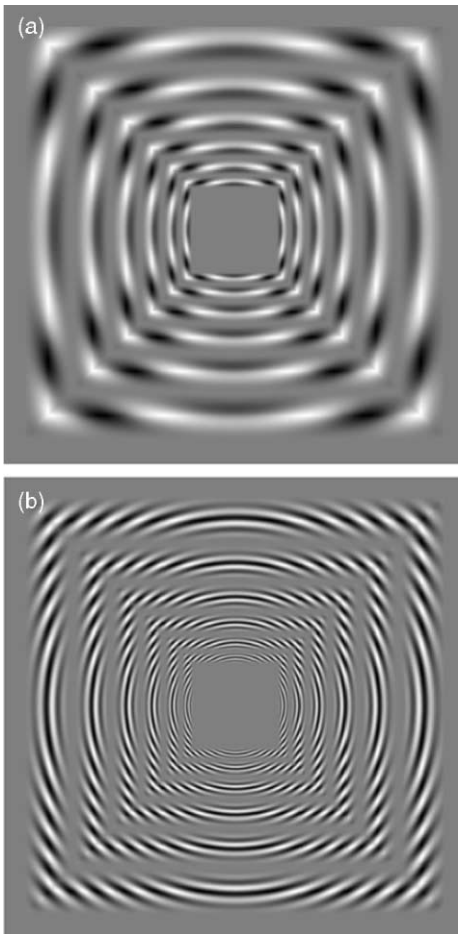

Fig. 6. Both figures comprise a radial carrier grating of (a) low and (b) high spatial frequency whose contrast is windowed by a series of squares. In (a) the squares appear "bowed outwards" in a convex direction illustrating the Fraser effect. In contrast, the squares in (b) appear "bowed inwards" in a concave manner demonstrating a Zöllner effect. Furthermore, the magnitude and direction of the illusion remains relatively constant within each figure, since the size of the squares varies simultaneously with the period of the carrier grating.

The perceived orientation of the contrast modulation was measured as a function of the orientation of the luminance grating. As the spatial frequency of the luminance modulation approached that of the contrast modulation, significant attractive effects were found at relative orientations up to 45°. Morgan et al. (2000) note that such a finding is unexpected, since conventional twisted-cord type stimuli produce a consistent repulsion effect at moderate values of relative orientation. Our data (Fig. 2) demonstrate that this discrepancy is a consequence of the relatively fine carrier spatial scale contained by conventional twisted-cord stimuli in comparison to the very coarse carrier scales which can be used in the type of stimuli used by McOwan and Johnston (1996).

We have chosen to demonstrate these spatial scale effects by varying the scale of the carrier against a fixed-size envelope. To reinforce our argument, we should point out that it is a simple matter to demonstrate similar effects by maintaining the carrier frequency and varying the envelope size.

Our viewing distance experiment also produced unequivocal results indicating that the attractive and repulsive effects of carrier orientation upon the envelope percept exhibit scale invariance. Since changes in viewing distance leave the spatial relationship between carrier and envelope unchanged, this result is further confirmation that this ratio is the decisive factor in determining the magnitude and direction of this kind of illusion. However, our result differs from the findings of Dakin et al. (1999), despite the use of similar stimuli.

They investigated changes in carrier spatial frequency for a 45° carrier orientation at three different viewing distances. The Zöllner-type effects that they find at this orientation appear to be similar across viewing distance when plotted in cycles per degree, rather than cycles per envelope. The reason for the differences between our study and that of Dakin et al. (1999) is unclear. Scale invariance can be confirmed by observation of the type of demonstration shown in Fig. 6a & b, where the reader should note the robustness of the illusions to changes in viewing distance.

The dependence of envelope judgements upon the nature of the carrier grating indicate that the recovery of 2nd-order structure by the visual system is imperfect, giving rise to the illusory effects which we have documented. As Dakin et al. (1999) point out, the interaction between carrier structure and envelope percept might occur at various sites. One possibility is that individual 2nd-order neurons are strictly tied to the orientation and scale of their 1st-order inputs. In this way, various combination schemes can be devised to introduce biases in the distribution of 2nd-order outputs consistent with psychophysical observations. In support of an early-stage interaction of this type, Dakin et al. (1999) note that this would be consistent with the lack of scale invariance which they find. Against this notion, however, is neurophysiological evidence, which suggests that there is no strict relationship between the spatial frequency and orientation characteristics of 2nd-order neurons and their 1st-order input (Mareschal & Baker, 1998; Zhou & Baker, 1996). An alternative suggestion is that the 1st-order luminance stream influences the output of the 2nd-order system at a relatively late stage (Morgan et al., 2000). This might occur at or subsequent to the level where the output of 2nd-order neurons is pooled to effectively synthesise circular filtering (Arsenault, Wilkinson, & Kingdom, 1999; McGraw et al., 1999). Current motion models also incorporate a late stage integration of 1st- and 2nd-order processing streams (Scott-Samuel & Georgeson, 1999; Wilson et al., 1992). In this way, the final 2nd-order orientation percept may be modulated by a combination of excitatory and inhibitory inputs from the 1st-order stream, the parameters of which depend critically upon relative spatial scale and orientation.

In summary, we have clarified several previous findings by quantifying perceptual interactions between 1st- and 2nd-order features as a function of both orientation *and* relative spatial scale. The critical importance of the relative spatial scale of carrier to envelope, and the associated scale invariance, represent findings which must be considered in models of 1st- and 2nd-order orientation processing. Analysis of the present data suggests that the effects are a consequence of a progressive reduction in inhibitory interactions between the band-pass carrier and the low-pass envelopes as the spatial scales of the two converge.

Acknowledgements

This work was supported by a Biomedical Research Collaboration Grant from the Wellcome Trust. PVM is supported by a Wellcome Trust Career Development Fellowship.

References

Arsenault, A. S., Wilkinson, F., & Kingdom, F. A. A. (1999). Modulation frequency and orientation tuning of second-order texture echanisms. *Journal of Optical Society of America A, 16*, 427–435.

Badcock, D. R., & Derrington, A. M. (1985). Detecting the displacement of periodic patterns. *Vision Research, 25*, 1253–1258.

Blakemore, C., Carpenter, R. H. S., & Georgeson, M. A. (1970). Lateral inhibition between orientation detectors in the human visual system. *Nature, 228*, 37–39.

Blakemore, C., & Tobin, A. E. (1972). Lateral inhibition between orientation detectors in the cat's visual cortex. *Experimental Brain Research, 15*, 439–440.

Burton, G. J. (1973). Evidence for nonlinear response processes in the human visual system from measurements on the thresholds of spatial beat frequencies. *Vision Research, 13*, 1211–1225.

Chubb, C., & Sperling, G. (1988). Drift-balanced random stimuli—a general basis for studying non-Fourier motion perception. *Journal of the Optical Society of America A, 5*, 1986–2007.

Dakin, S. C., & Mareschal, I. (2000). Sensitivity to amplitude modulation depends on carrier spatial frequency and orientation. *Vision Research, 40*, 311–329.

Dakin, S. C., Williams, C. B., & Hess, R. F. (1999). The interaction of first- and second-order cues to orientation. *Vision Research, 39*, 2867–2884.

DeValois, R. L., Albrecht, D. G., & Thorell, L. G. (1982). Spatial frequency selectivity of cells in macaque visual cortex. *Vision Research, 22*, 545–559.

Edwards, M., & Badcock, D. R. (1995). Global motion perception—no interaction between first and second order motion pathways. *Vision Research, 35*, 2589–2602.

Fraser, J. (1908). A new illusion of visual direction. *British Journal of Psychology, 2*, 307–320.

Ferster, D. (1986). Orientation selectivity of synaptic potentials in neurons of cat primary visual cortex. *Journal of Neuroscience, 6*, 1284–1301.

Henning, G. B., Hertz, B., & Broadbent, D. E. (1975). Some experiments bearing on the hypothesis that the visual system analyses patterns in independent bands of spatial frequency. *Vision Research, 15*, 887–899.

von der Heydt, R., & Peterhans, E. (1989). Mechanisms of contour perception in monkey visual cortex. 1. Lines of pattern discontinuity. *Journal of Neuroscience, 9*, 1731–1748.

Hubel, D. H., & Weisel, T. N. (1959). Receptive fields of single neurons in the cat striate cortex. *Journal of Physiology, 148*, 574–591.

Langley, K., Fleet, D. J., & Hibbard, P. B. (1999). Stereopsis from contrast envelopes. *Vision Research, 39*, 2313–2324.

Ledgeway, T., & Smith, A. T. (1994). Evidence for separate motion detection mechanisms for first- and second-order motion in human vision. *Vision Research, 34*, 2727–2740.

Lin, L. M., & Wilson, H. R. (1996). Fourier and non-Fourier pattern discrimination compared. *Vision Research, 36*, 1907–1918.

Mareschal, I., & Baker, C. L. (1998). A cortical locus for the processing of contrast-defined contours. *Nature Neuroscience, 1*, 150–154.

McGraw, P. V., Levi, D. M., & Whitaker, D. (1999). Spatial characteristics of the second-order visual pathway revealed by positional adaptation. *Nature Neuroscience, 2*, 479–484.

McOwan, P. W., & Johnston, A. (1996). A second-order pattern reveals separate strategies for encoding orientation in two-dimensional space and space-time. *Vision Research, 36*, 425–430.

Morgan, M. J., & Baldassi, S. (1997). How the visual system encodes the orientation of a texture and why it makes mistakes. *Current Biology, 7*, 999–1002.

Morgan, M. J., Mason, A. J. S., & Baldassi, S. (2000). Are there separate first-order and second-order mechanisms for orientation discrimination? *Vision Research, 40*, 1751–1763.

Movshon, J. A., Thompson, J. A., & Tolhurst, D. J. (1978). Spatial summation in the receptive fields of simple cells in the cat's striate cortex. *Journal of Physiology, 283*, 53–77.

Paradiso, M. A. (1988). A theory for the use of visual orientation information which exploits the columnar structure of striate cortex. *Biological Cybernetics, 58*, 35–49.

Pelli, D. G., & Zhang, L. (1991). Accurate control of contrast on micro-computer displays. *Vision Research, 31*, 1337–1350.

Popple, A. V., & Levi, D. M. (2000). A new illusion demonstrates long range processing. *Vision Research, 40*, 2545–2549.

Ringach, D. L. (1998). Tuning of orientation detectors in human vision. *Vision Research, 38*, 963–972.

Scott-Samuel, N. E., & Georgeson, M. A. (1999). Does early non-linearity account for second-order motion? *Vision Research, 39*, 2853–2865.

Shapley, R. M. (1994). Linearity and non-linearity in cortical receptive fields. *CIBA Foundation Symposium, Higher-order Processing in the Visual System* (vol. 184, pp. 71–81). Chichester: Wiley.

Smith, S., Clifford, C. W. G., & Wenderoth, P. (2001). Interaction between first- and second-order orientation channels revealed by the tilt illusion: psychophysics and computational modelling. *Vision Research, 41*, 1057–1071.

Spitzer, H., & Hochstein, L. I. (1985). Simple-cell and complex-cell response dependencies on stimulation parameters. *Journal of Neurophysiology, 53*, 1244–1265.

Sutter, A., Sperling, G., & Chubb, C. (1995). Measuring the spatial-frequency selectivity of 2nd-order texture mechanisms. *Vision Research, 35*, 915–924.

Tyler, C. W., & Nakayama, K. (1984). Size interactions in the perception of orientation. In L. Spillman & B. R. Wooton (Eds.), *Sensory experience, adaptation and perception* (pp. 529–546). Earlbaum, NJ: Hillsdale.

Wenderoth, P., Clifford, C. W. G., & Wyatt, A. M. (2001). Hierarchy of interactions in the processing of contrast-defined contours. *Journal of Optical Society of America A, 18*, 2190–2196.

Whitaker, D., McGraw, P. V., & Levi, D. M. (1997). The influence of adaptation on perceived visual location. *Vision Research, 37*, 2207–2216.

Wilson, H. R., Ferrera, P., & Yo, C. (1992). A psychophysically motivated model for two dimensional motion perception. *Visual Neuroscience, 9*, 79–97.

Wilson, H. R., & Richards, W. A. (1992). Curvature and separation discrimination at texture boundaries. *Journal of the Optical Society of America A, 9*, 1653–1662.

Zeigler, L. R., & Hess, R. F. (1999). Stereoscopic depth but not shape perception from second order stimuli. *Vision Research, 39*, 1491–1507.

Zhou, Y. X., & Baker, C. L. (1996). Spatial properties of envelope responsive cells in area 17 and 18 neurons of the cat. *Journal of Neurophysiology, 75*, 1038–1050.